NUKLEONIKA 2015;60(4):759–763
doi: 10.1515/nuka-2015-0137

ORIGINAL PAPER

DE GRUYTER
OPEN

Understanding electron-positron momentum densities in solids: effect of the positron distribution

Anna Rubaszek

Abstract. The influence of the positron distribution on the electron-positron (e-p) momentum densities (MDs) is studied in terms of the l ($l = s, p, d, f$) character of the initial electronic state. The effect of the positron is discussed for momenta in the extended and reduced zone scheme on the example of Al (simple metal), Cu (metal with almost filled d shell), and Cr (transition metal). Present result indicates a weak sensitivity of the e-p MD inside the central Fermi surface to the positron charge density for the delocalized s and p electrons. In the case of d states, the effect of the positron on the relevant contribution to the e-p MD directly reflects the degree of localization of d electrons in the electron density of states.

Key words: positron annihilation • electronic band structure • positron states

Introduction

The positron annihilation spectroscopy is a sensitive technique to probe the electronic properties of solids [1–4]. In particular, the angular correlation of the positron annihilation radiation and coincidence Doppler broadening (DB) spectra carry a useful information on the electron momentum density (EMD) in the host material, $\rho^{\mathrm{EMD}}(\mathbf{p})$. This information is, however, modified by two effects: the strong many-body e-p interaction and deviation of the positron wave function, $\psi_+(\mathbf{r})$, from the single plane wave, associated with momentum $\mathbf{k}_+ = 0$. The sensitivity of the e-p MD to the e-p correlations is discussed elsewhere ([5] and references cited therein). The present contribution is devoted to the study of the second effect. Here the e-p momentum density (MD) calculated within the independent particle model (IPM), $\rho^{\mathrm{IPM}}(\mathbf{p})$, serves as a good reference point, in spite of its purely theoretical character. The relevant independent particle model factor (IPMF), $\varepsilon^{\mathrm{IPM}}(\mathbf{p}) = \rho^{\mathrm{IPM}}(\mathbf{p})/\rho^{\mathrm{EMD}}(\mathbf{p})$, gives a direct account for the influence of the positron distribution on the resulting MDs.

A. Rubaszek
W. Trzebiatowski Institute of Low Temperatures and Structure Research, Polish Academy of Sciences, P. O. Box 1410, 50-950 Wrocław 2, Poland,
Tel.: +48 71 395 4272, Fax: +48 71 344 1029,
E-mail: A.Rubaszek@int.pan.wroc.pl

Received: 22 June 2015
Accepted: 12 August 2015

The EMD and e-p IPM MD read as

$$\rho^{\mathrm{EMD}}(\mathbf{p}=\mathbf{k}+\mathbf{G})=\sum_j \rho_j^{\mathrm{EMD}}(\mathbf{p}) = \sum_j \theta_{\mathbf{k}j}/\Omega \left|\int_\Omega e^{-i\mathbf{p}\cdot\mathbf{r}}\psi_{\mathbf{k}j}(\mathbf{r})d\mathbf{r}\right|^2 \quad (1)$$

$$\rho^{\mathrm{IPM}}(\mathbf{p}=\mathbf{k}+\mathbf{G})=\sum_j \rho_j^{\mathrm{IPM}}(\mathbf{p}) = \sum_j \theta_{\mathbf{k}j}\left|\int_\Omega e^{-i\mathbf{p}\cdot\mathbf{r}}\psi_{\mathbf{k}j}(\mathbf{r})\psi_+(\mathbf{r})d\mathbf{r}\right|^2$$

where $\mathbf{p}$ and $\mathbf{k}$ are the momenta in the extended and reduced zone scheme, respectively; $\mathbf{G}$ denotes the reciprocal lattice vector; $\theta_{\mathbf{k}j}$ and $\psi_{\mathbf{k}j}(\mathbf{r})$ are the occupation number and wave function of the initial electron Bloch state $\mathbf{k}j$ (associated with the wave vector $\mathbf{k}$ and band index j), respectively; and Ω is the volume of the unit cell. After folding, the spectra to the first Brillouin zone (BZ) within the Lock-Crisp-West (LCW) procedure [6], the IPM MD in the band j takes the form

$$\rho_{\mathrm{LCW}}^{\mathrm{IPM}}(\mathbf{k}j)=\sum_{\mathbf{G}}\rho_j^{\mathrm{IPM}}(\mathbf{k}+\mathbf{G}) = \Omega\theta_{\mathbf{k}j}\int_\Omega |\psi_{\mathbf{k}j}(\mathbf{r})|^2 |\psi_+(\mathbf{r})|^2\, d\mathbf{r}. \quad (2)$$

As the corresponding EMD reduces to the occupation number, $\theta_{\mathbf{k}j}$, the LCW IPMF in the band j is exactly equal to the relevant IPM MD, $\rho_{\mathrm{LCW}}^{\mathrm{IPM}}(\mathbf{k}j)$.

Authors of Refs. [7–9] discussed the effect of the positron distribution and many-body effects on the leading and high-momentum components (HMC) of the e-p MD in simple and transition metals. In the present work, we study the influence of the positron wave function on the e-p spectra within an alternative approach on the example of Al, Cu, and Cr. In particular, the change in the contributions from the *s*, *p*, and *d* electrons to the e-p MDs is investigated also as a function of energy of annihilating electron.

Results and discussion

Electron and positron wave functions, incorporated in Eqs. (1) and (2), have been calculated within the muffin-tin orbital atomic sphere approximation (MTO-ASA) band structure method [10, 11]. The electron wave functions inside the atomic sphere approximation (ASA) are assumed in the form

$$\psi_{\mathbf{k}j}(\mathbf{r})=\sum_{l,m} i^l Y_{lm}(\mathbf{r})A_{lm}^{\mathbf{k}j}\phi_l(E_{\mathbf{k}j},r) \quad (3)$$

where Y_{lm} denotes the spherical harmonics and $E_{\mathbf{k}j}$, A, and ϕ_l are, respectively, the energies, eigen values, and spherical solutions of the electron Schrödinger equation. The positron wave function has predominantly $l = s$ character. The relevant e-p MDs in the extended and reduced zone scheme are given by the formulas

$$\rho^{\mathrm{IPM}}(\mathbf{p}=\mathbf{k}+\mathbf{G})=\sum_j \theta_{\mathbf{k}j}\left|\sum_{l,m} Y_{lm}(\mathbf{k}+\mathbf{G})A_{lm}^{\mathbf{k}j}\int_\Omega r^2 j_l(pr)\phi_l(E_{\mathbf{k}j},r)\psi_+(r)dr\right|^2 \quad (4)$$

$$\rho_{\mathrm{LCW}}^{\mathrm{IPM}}(\mathbf{k}j)=\sum_l \rho_{\mathrm{LCW}}^{\mathrm{IPM}}(\mathbf{k}j,l) = \Omega\theta_{\mathbf{k}j}\sum_{l,m}\left|A_{lm}^{\mathbf{k}j}\right|^2\int_\Omega r^2\left|\phi_l(E_{\mathbf{k}j},r)\right|^2\left|\psi_+(r)\right|^2 dr$$

where $j_l(pr)$ are the spherical Bessel functions. The EMD corresponds to applying $\psi_+ = \Omega^{-1/2}$ in Eq. (4). It is worth to point out here the essential difference between the basic features of the e-p MDs in the reduced and extended zone scheme. First, for momenta $\mathbf{p}$ along a fixed crystallographic direction, only some electron bands (well determined by the symmetry rules [12]) contribute to the EMD and e-p MD in the extended zone scheme, while the Fermi surface (FS) breaks from the all occupied electron bands exhibit in the spectra folded to the first BZ. Second, there is a strong hybridization of the contributions

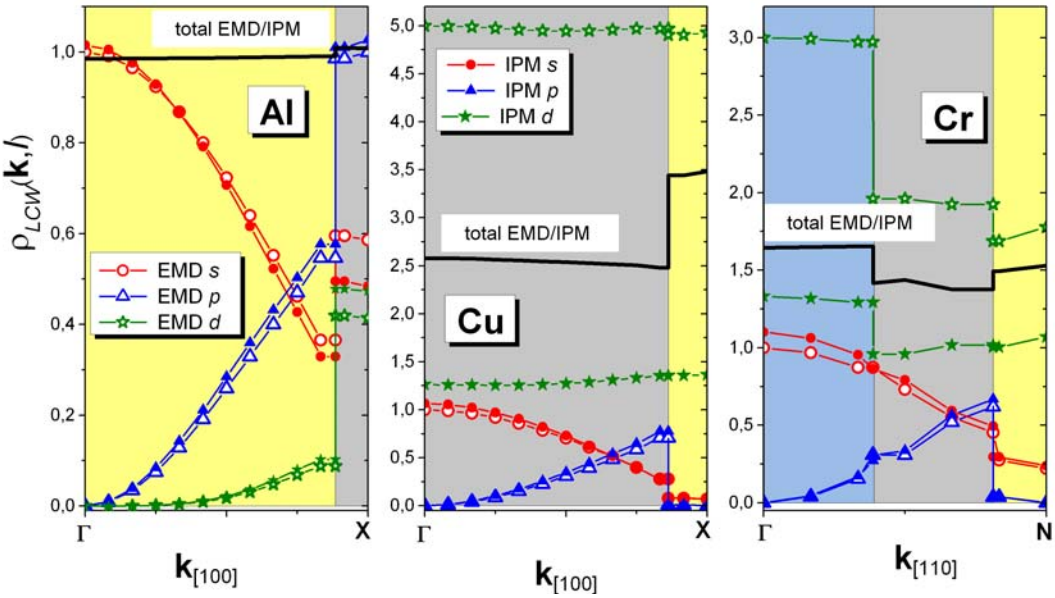

Fig. 1. The LCW-folded EMD (open symbols) and IPM MDs (full symbols) along the [100] direction decomposed into the *s* (circles), *p* (triangles), and *d* (stars) waves. The inverse of the total IPMF, $1/\varepsilon_{\mathrm{LCW}}^{\mathrm{IPM}}(\mathbf{k})$, is marked by a solid line.

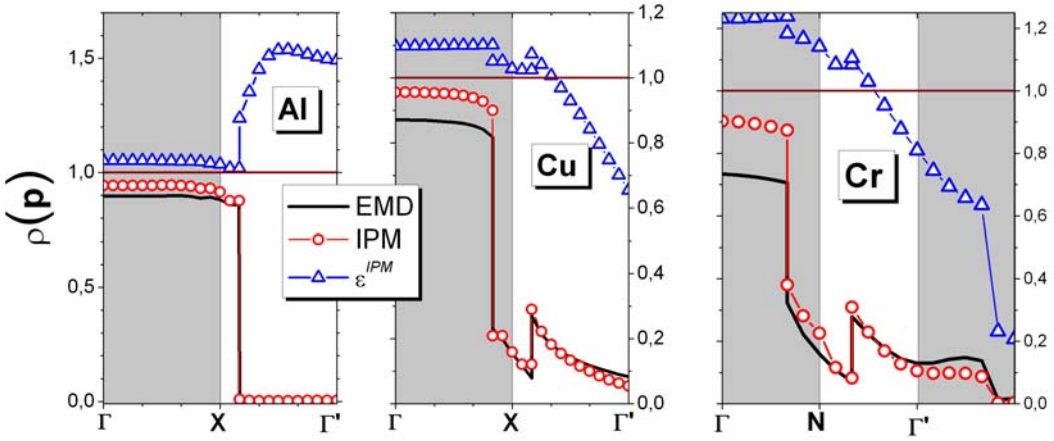

Fig. 2. The EMD (solid lines), e-p IPM MD (circles), and IPMF (triangles) for momenta in the extended zone scheme along the main crystallographic directions.

from the *s*, *p*, and *d* electrons, observed in the MDs in the extended zone scheme, while these contributions are easily separable in the LCW-folded spectra, as it follows from Eq. (4). This fact is illustrated in Fig. 1 for Al, Cu, and Cr. The last point is that the IPMF in the extended zone scheme is strongly momentum dependent in the high-momentum region, as it is visualized in Fig. 2. In contrast to $\rho^{\mathrm{EMD/IPM}}(\mathbf{p})$, for a fixed crystallographic direction, the LCW-folded densities exhibit a momentum dependence only in particular bands (these ones, which give contribution to the EMD along this direction in the extended zone scheme [12]). It is worth to note that the total density is hardly momentum dependent, except the FS breaks, as it can be seen in Figs. 1 and 3. These features are discussed in Refs. [7–9] and they are attributed to the overlap of bands of *s*, *p*, and *d* character.

In order to study the effect of the positron wave function on the $l = s, p, d$ states, we introduce the l character and energy-dependent IPMF,

$$\varepsilon^{\mathrm{IPM}}(E,l) = \sum_{\mathbf{k}j} \delta(E - E_{\mathbf{k}j}) \rho^{\mathrm{IPM}}_{\mathrm{LCW}}(\mathbf{k}j,l) / N_l(E)$$
$$N_l(E) = \sum_{\mathbf{k}j} \delta(E - E_{\mathbf{k}j}) \rho^{\mathrm{EMD}}_{\mathrm{LCW}}(\mathbf{k}j,l) \quad (5)$$

where $N_l(E)$ is the l component of the electron density of states in the host material. The parameter $\varepsilon^{\mathrm{IPM}}(E,l)$ is plotted in Fig. 4 for Al, Cu, and Cr. The first thing to note is that $\varepsilon^{\mathrm{IPM}}(E,l)$ is a decreasing function of energy for all types of electrons. The negative slope of the individual curves depends on the degree of localization of electrons, and it is most pronounced for *d* electrons in Cu. The quantitative behavior of $\varepsilon^{\mathrm{IPM}}(E,l)$ in the *d*-electron metals is essentially different as compared to the electron-gas-like aluminum, especially for *d* electrons. In copper and chromium, the overlap of the positron density with *d* electrons is considerably reduced as compared to the uniform positron distribution. In contrast to transition metals, for Al, the values of $\varepsilon^{\mathrm{IPM}}(E,d)$ are 10–20% larger than unity. This feature can be directly attributed to the degree of localization of

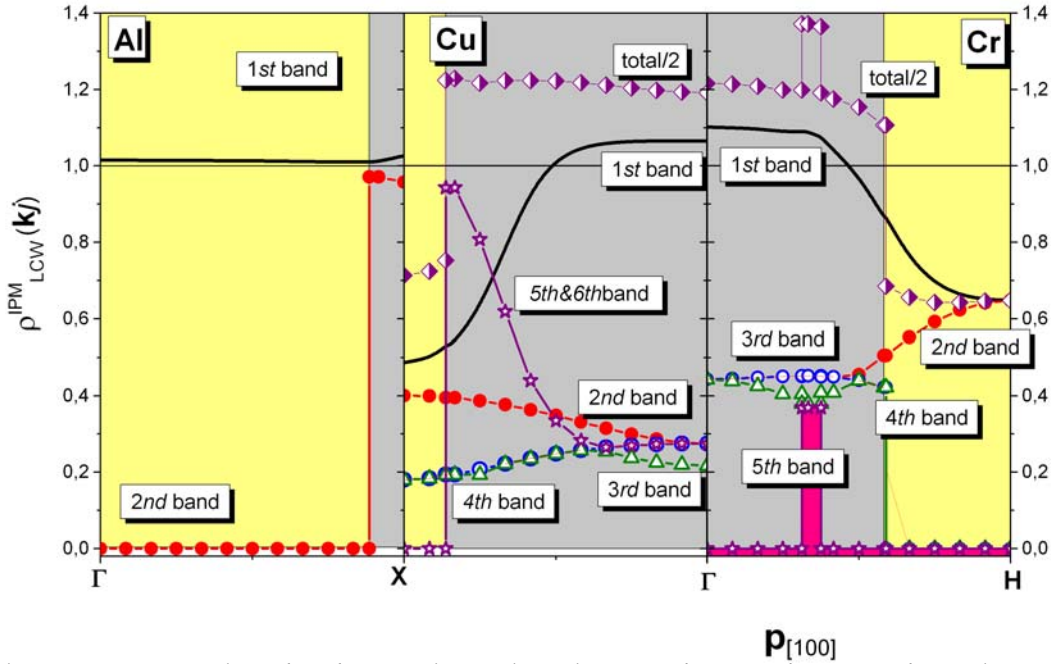

Fig. 3. The e-p IPM MD in the reduced zone scheme along the [100] direction decomposed into the contributions from individual bands. Diamonds refer to the total MD multiplied by a factor 0.5.

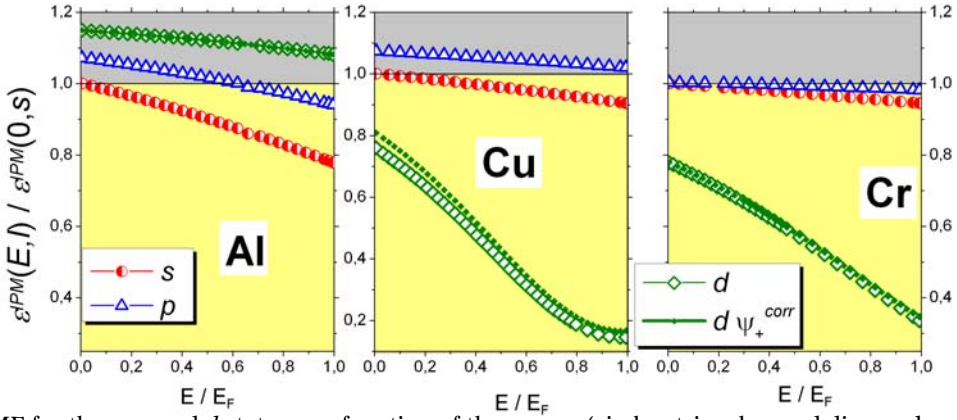

Fig. 4. The IPMF for the *s*, *p*, and *d* states as a function of the energy (circles, triangles, and diamonds, respectively). Zero energy is set at the bottom of the valence band. ψ_+^{LDA} (stars) refers to the non-zero electron-positron correlation potential in the positron model.

d states in elements under study. Application of the e-p interaction potential in the positron model increases the values of $\varepsilon^{IPM}(E,d)$ close to the Fermi energy very slightly, and it is hardly observed for *s* and *p* electrons. The IPMF for *p* states is greater than unity in the whole energy range. The only exception are the electrons close to the Fermi energy in Al. The IPMF of *s* electrons is smaller than its *p* counterpart. The values of $\varepsilon^{IPM}(E,s)$ at the Fermi level fall below unity in Cr, Cu, and Al.

The above properties of $\varepsilon^{IPM}(E,l)$ are directly transferred to the e-p MDs and IPMFs for momenta both in the extended and reduced zone scheme. The IPMF in the extended zone scheme, $\varepsilon^{IPM}(\mathbf{p})$ shown in Fig. 2, is not strongly momentum dependent inside the central FS, in contrast to its components from the individual bands *j*. For Cu and Cr, the parameter $\varepsilon^{IPM}(\mathbf{p})$ slightly increases toward the Fermi momentum (or the BZ boundary) in the low-momentum region, and it exhibits strongly decreasing slope in the higher BZs, dominated by *d* states. Generally, for transition and noble metals, this is the *d* electrons' contribution to the EMD and DOS (as can be seen in Fig. 4), which is responsible for strong decrease in the relevant IPMF in the high-momentum region. This fact is illustrated for Cu and Cr in Fig. 2. In contrast to Cu and Cr, the IPMF in Al slightly decreases toward the FS. Furthermore, a large overenhancement, because of *p* (and partially *d*) electrons in Al, is observed in the second BZ for momenta above the Fermi momentum. This overenhancement is common for all the alkali metals (however, only for the 'first' HMC as shown in Refs. [7–9]), characterized by the *p* like HMCs of the EMD.

The LCW-folded EMD and IPM MDs in Al, Cu, and Cr decomposed into the contributions from the partial waves are shown in Fig. 1. The total IPMF and MD are presented in Figs. 1 and 3, respectively. In order to keep in the figures scale, in Fig. 1, the inverse of the total IPMF is plotted instead of the direct parameter and the $\rho_{LCW}^{IPM}(\mathbf{k})$ is divided by 2 in Fig. 3. In all the elements under study, the *s* electrons' contribution decreases toward the BZ boundary, while *p* electrons part shows an increasing tendency. The relevant IPMFs are hardly momentum dependent and greater than unity. The only exception are the *s* electrons in Al (see also Fig. 4). Except for Al, the *d* electrons' contribution to EMD is strongly reduced by the positron wave function. The *d* component of the EMD and IPM MD is hardly momentum dependent between the FS breaks, similar to the IPMF.

The (rather strong) momentum dependence of the *s* and *p* parts compensate one another and the resulting total IPM MD reproduces the slope of the total EMD. In consequence, the total IPMF exhibits rather weak-momentum dependent between the FS breaks. One can also see in Figs. 1 and 3 that the height of the steps in the EMD at the FS (equal to unity) is essentially reduced in the IPM spectrum by the positron wave function.

The contributions from individual bands to the LCW-folded IPM MD in Al, Cu, and Cr are displayed in Fig. 3 for momenta **k** along the [100] direction. The slope of $\rho_{LCW}^{IPM}(\mathbf{k}j)$ reflects directly increasing or decreasing *d* character of the band *j*. For this reason, the behavior of the $\rho_{LCW}^{IPM}(\mathbf{k}j)$ in Cu and Cr is very similar, while a nearly free character of the electron bands in Al (and, generally, in simple metals) leads to hardly momentum-dependent LCW-folded IPM MD.

Conclusions

In summary, one can say that in transition and noble metals, the contribution from the localized *d* electrons is essentially reduced in the e-p MD by the positron wave function, while in the nearly free electron systems, such as alkalis and Al, *d* electrons are well delocalized and their contribution to the e-p MD is increased by a positron. The contribution from *p* states is generally increased in the e-p MD as compared to the EMD, while the *s* electrons are less sensitive to the positron distribution. Furthermore, the positron wave function hardly affects the e-p MD inside the central FS, while its effect on the HMCs strongly depends on the character and degree of localization of electrons contributing to the EMD in this region. The total IPMF for the spectra folded to the first BZ is essentially less-momentum dependent than its counterpart in the extended zone scheme. The momentum dependence of the IPMF for the LCW-folded spectra is observed only

after decomposition into the contributions either from the individual bands or from the $l = s, p, d, f$ partial waves.

Finally, one should pay some attention to the HMCs of the e-p MDs, discussed in several papers [7–9]. It is well known that the HMCs of the MDs are dominated by *d* electrons with a small fraction of *p* states. Therefore, there is an essential difference between HMCs in Al and transition metals, because of the different degree of localization of *d* electrons in the electron density of states. In Al, the delocalized *d* states are overenhanced in the whole energy range, while *d* states in transition metals are strongly de-enhanced. Furthermore, *p* electrons in Al are overenhanced by a positron only for low energies. In consequence, HMCs in transition metals are generally de-enhanced. In contrast to transition metals, in Al, both the overenhancement and de-enhancement of HMCs are observed, depending on the degree of hybridization of the *p* and *d* states and energies of the annihilating Bloch states.

References

1. Puska, M. J., & Nieminen, R. M. (1994). Theory of positrons in solids and on solid surfaces. *Rev. Mod. Phys*., *66*, 841–898. DOI: 10.1103/RevModPhys.66.841.
2. Nieminen, R. M. (1996). Positrons in solids. In A. Dupasquier, & A. P. Mills (Eds.), *Positron spectroscopy of solids* (pp. 443–465). Amsterdam: IOP Press.
3. West, R. N. (1974). *Positron studies of condensed matter*. London: Taylor and Francis.
4. Berko, S. (1983). Momentum density and Fermi surface measurements in metals by positron annihilation. In W. Brandt, & A. Dupasquier (Eds.), *Positron solid state physics* (pp. 64–145). Amsterdam: North-Holland Publ. Co.
5. Rubaszek, A. (2015). Insight into the electron-positron correlations in solids. Submitted to *Physica B* [and references cited therein].
6. Lock, D. G., Crisp, V. H. C., & West, R. N. (1973). Positron annihilation and Fermi surface studies: a new approach. *J. Phys. F-Met. Phys*., *3*, 561–570. http://iopscience.iop.org/0305-4608/3/3/014/pdf/0305-4608_3_3_014.pdf.
7. Kontrym-Sznajd, G., Sormann, H., & Boroński, E. (2012). General properties of electron-positron momentum densities. *Phys. Rev. B*, *85*, 24510(9 pp.). DOI: 10.1103/PhysRevB.85.245104 [and references cited therein].
8. Kontrym-Sznajd, G., & Sormann, H. (2014). The influence of a positron on electron-positron momentum densities in metallic materials. *Phys. Scripta*, *89*, 015808(7 pp.). DOI: 10.1088/0031-8949/89/01/015808 [and references cited therein].
9. Kontrym-Sznajd, G., & Rubaszek, A. (1993). Interpretation of positron annihilation data with respect to the electron-positron momentum densities. *Phys. Rev. B*, *47*, 6950–6970. DOI: 10.1103/PhysRevB.47.6950.
10. Andersen, O. K. (1975). Linear methods in bands theory. *Phys. Rev. B*, *12*, 3060–3083. DOI: 10.1103/PhysRevB.12.3060.
11. Skriver, H. L. (1984). *The LMTO method. Muffin-tin orbitals and electronic structure*. Berlin: Springer-Verlag.
12. Harthoorn, P., & Mijnarends, P. E. (1978). The effect of symmetry on electron momentum densities in solids. *J. Phys. F-Met. Phys*., *8*, 1147–1158. http://iopscience.iop.org/0305-4608/8/6/016/pdf/0305-4608_8_6_016.pdf .